Bax/Bak promote sumoylation of DRP1 and its stable association with mitochondria during apoptotic cell death

Sylwia Wasiak, Rodolfo Zunino, and Heidi M. McBride

University of Ottawa Heart Institute, Ottawa, Ontario K1Y 4W7, Canada

Dynamin-related protein 1 (DRP1) plays an important role in mitochondrial fission at steady state and during apoptosis. Using fluorescence recovery after photobleaching, we demonstrate that in healthy cells, yellow fluorescent protein (YFP)–DRP1 recycles between the cytoplasm and mitochondria with a half-time of 50 s. Strikingly, during apoptotic cell death, YFP-DRP1 undergoes a transition from rapid recycling to stable membrane association. The rapid cycling phase that characterizes the early stages of apoptosis is independent of Bax/Bak. However, after Bax recruitment to the mitochondrial membranes but before the loss of mitochondrial membrane potential, YFP-DRP1 becomes locked on the membrane, resulting in undetectable fluorescence recovery. This second phase in DRP1 cycling is dependent on the presence of Bax/Bak but independent of hFis1 and mitochondrial fragmentation. Coincident with Bax activation, we detect a Bax/Bak-dependent stimulation of small ubiquitin-like modifier-1 conjugation to DRP1, a modification that correlates with the stable association of DRP1 with mitochondrial membranes. Altogether, these data demonstrate that the apoptotic machinery regulates the biochemical properties of DRP1 during cell death.

Introduction

Mitochondrial shapes range from interconnected networks to punctiform organelles in different cell types. Recent experiments have demonstrated that the mitochondrial morphology is an important determinant of mitochondrial function (McBride et al., 2006). In fact, the mitochondrial reticulum can be rapidly remodeled by dynamic fission and fusion events in response to the physiological requirements of a cell (Chan, 2006). For example, extensive mitochondrial fragmentation is observed during apoptotic cell death and in hyperglycemic conditions (Frank et al., 2001; Yu et al., 2006).

Mitochondrial fission and fusion rely on the function of multiple proteins that mediate the remodeling of the outer and inner mitochondrial membrane (Okamoto and Shaw, 2005). In mammalian cells, fission requires dynamin-related protein 1 (DRP1; Smirnova et al., 2001; Yoon et al., 2001) along with hFis1 (James et al., 2003; Yoon et al., 2003; Stojanovski et al., 2004), endophilin B1/Bif-1 (Karbowski et al., 2004; Takahashi et al., 2005), MTP18 (Tondera et al., 2005), GDAP1 (Niemann et al., 2005), DAP3 (Mukamel and Kimchi, 2004), and potentially other unknown proteins. Similar to other dynamins, DRP1 and its yeast orthologue Dnm1p contain an N-terminal GTPase domain, a coiled-coil middle domain involved in protein self-assembly, and a C-terminal GTPase-activating domain (Fukushima et al., 2001; Pitts et al., 2004; Zhu et al., 2004; Ingerman et al., 2005). In vitro, DRP1 forms oligomeric ringlike structures and tubulates liposomes in a nucleotide-dependent manner, suggesting that it functions directly in membrane constriction and/or scission (Yoon et al., 2001). In vivo, DRP1 forms cytosolic tetramers and is recruited to defined loci along the mitochondrial surface, which often mark sites of mitochondrial fission (Shin et al., 1999; Smirnova et al., 2001; Pitts et al., 2004; Zhu et al., 2004). The function of mitochondrial DRP1 puncta that are not associated with active constriction sites is unclear.

The recruitment of DRP1 from the cytosol to the mitochondrial surface is likely mediated by membrane-associated receptors. Three proteins—Fis1p, Mdv1p, and Caf4p—have been described to form a complex with Dnm1p (Mozdy et al., 2000; Tieu et al., 2002; Cerveny and Jensen, 2003; Griffin et al., 2005; Karren et al., 2005; Bhar et al., 2006; Naylor

Correspondence to Heidi M. McBride: hmcbride@ottawaheart.ca

Abbreviations used in this paper: BMK, baby mouse kidney; DKO, double knockout; DRP1, dynamin-related protein 1; STS, staurosporin; SUMO, small ubiquitin-like modifier; WT, wild type.

The online version of this article contains supplemental material.

The Journal of Cell Biology, Vol. 177, No. 3, May 7, 2007 439–450
http://www.jcb.org/cgi/doi/10.1083/jcb.200610042

et al., 2006; Schauss et al., 2006). In mammalian cells, only the outer membrane protein hFis1 has been proposed to fulfill this function, and evidence suggests that the nature of this complex is rather transient (Yoon et al., 2003; Yu et al., 2005). However, given the uniform distribution of hFis1p on the mitochondrial surface and the fact that its removal does not alter the recruitment of DRP1 to mitochondria (Lee et al., 2004; Stojanovski et al., 2004), it is likely that other factors contribute to DRP1 assembly and/or function. For instance, sumoylation and ubiquitination were recently reported as potential regulators of the DRP1 activity (Harder et al., 2004; Nakamura et al., 2006; Yonashiro et al., 2006). Components of the sumoylation machinery have also been reported to modulate the oligomerization and function of dynamin 1 (Mishra et al., 2004), suggesting that this posttranslational modification may control the activity of several members of the dynamin family of GTPases.

Recent evidence indicates that DRP1 participates in mitochondrial fission during apoptotic cell death (Frank et al., 2001; Breckenridge et al., 2003; Lee et al., 2004; Germain et al., 2005; Parone et al., 2006). Interference with DRP1 function during apoptosis results in a block of mitochondrial fission, leading to long interconnected organelles, as well as a delay in cell death. Mitochondrial fission is an early apoptotic event, occurring within the same time frame as activation of the pro-apoptotic Bcl-2 family member Bax and permeabilization of the mitochondrial outer membrane that leads to the release of multiple inner membrane space proteins and loss of the mitochondrial membrane potential ($\Delta\Psi$; for reviews see Heath-Engel and Shore, 2006; Martinou and Youle, 2006). It is presently unclear how a fission-mediating GTPase such as DRP1 is integrated into this series of events. Down-regulation of DRP1 expression by RNAi or overexpression of a dominant-negative mutant DRP1 K38A delays but does not block Bax recruitment and activation on the mitochondrial membranes and inhibits cytochrome *c* release from mitochondria (Frank et al., 2001; Lee et al., 2004; Neuspiel et al., 2005; Parone et al., 2006). This implies that both Bax and DRP1 function upstream of cytochrome *c* release in the apoptotic cascade of events, with DRP1 potentially participating in efficient Bax activation. Importantly, the overexpression of DRP1 K38E blocks remodeling of the mitochondrial cristae (Germain et al., 2005), an event that allows for the translocation of cytochrome *c* from the intracristal stores to the intermembrane space, from where it is released (Scorrano et al., 2002; Germain et al., 2005). This is consistent with recent data indicating that interference with DRP1 function does not affect the release of SMAC (second mitochondria-derived activator of caspases)/Diablo, which resides in the intermembrane space, but strongly inhibits the release of cytochrome *c* that is mostly confined to cristae (Arnoult et al., 2005; Parone et al., 2006). Whether DRP1-mediated fission is coupled to inner membrane remodeling or whether DRP1 has a more direct function in cristae remodeling remains to be determined.

Although it has been established that the membrane remodeling machinery participates in apoptosis, two important questions remain. First, it is unclear whether the process of fragmentation or alterations in membrane curvature (including cristae remodeling) are requisite for apoptosis. Second, it remains unclear how the fission proteins are activated by the apoptotic machinery. It has been observed that mitochondria-associated Bax coalesces at DRP1-containing fission sites and mitochondrial tips during cell death, implying that they may function together in membrane remodeling (Karbowski et al., 2002). On the other hand, colocalization between Bax and Mfn2, a GTPase involved in mitochondrial fusion, may account for a block in fusion observed during apoptosis (Karbowski et al., 2002). The link between the fusion machinery and Bax was recently highlighted by the discovery that Bax is required for the regulation of Mfn2 activity and lateral assembly into foci along the mitochondrial tubules (Karbowski et al., 2006). Also, upon apoptotic stimulus, endophilin B1/Bif-1, a membrane-shaping protein, has been reported to interact with Bax and to control the recruitment and activation of both Bax and Bak, another

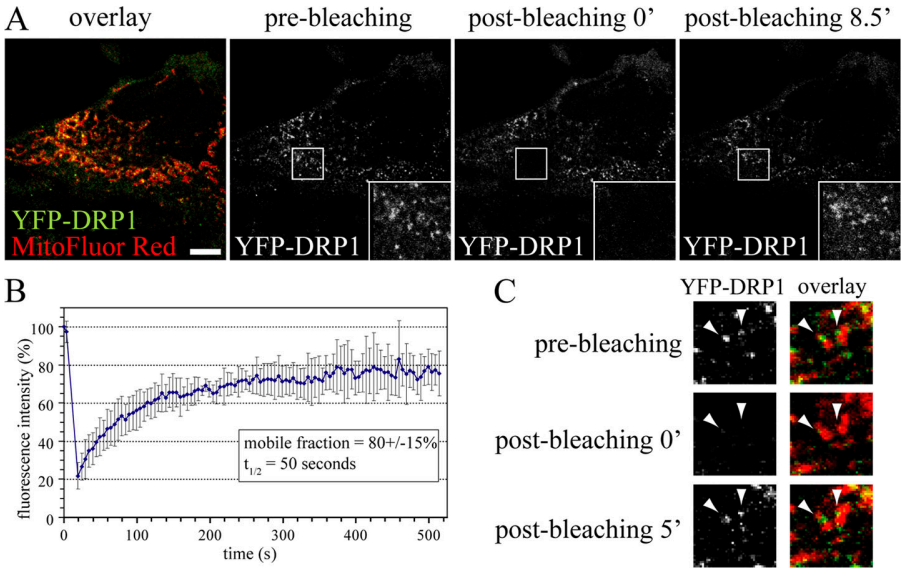

Figure 1. **YFP-DRP1 rapidly cycles between the cytosol and preexisting sites on the mitochondrial membranes.** (A) HeLa cells were transfected with YFP-DRP1 and Oct-DsRed (overlay). The boxed regions containing YFP-DRP1 staining (insets) associated with mitochondria was photobleached (0 min), and fluorescence recovery was monitored over time (8.5 min). Bar, 5 μm. (B) Relative fluorescence intensity of YFP-DRP1 recorded during a photobleaching protocol was plotted as a function of time ($n = 7$ cells). Equations used to calculate these parameters are described in Materials and methods. Error bars represent SD. (C) YFP-DRP1 (green) localized to mitochondria labeled with the MitoFluor red dye (red) was photobleached (0 min), and the fluorescence recovery was monitored over time (5 min). Arrowheads indicate recovery to the same puncta.

Bcl-2–like homologue (Karbowski et al., 2004; Takahashi et al., 2005). It is conceivable that channel-forming properties of Bax are actually regulated by changes in membrane shape induced by endophilin B1/Bif-1, although this hypothesis needs to be explored further.

Because the fission/fusion proteins also function at steady state, their properties are likely to be altered during cell death, allowing them to participate in membrane remodeling that is specific for the mitochondrial apoptotic pathway. In fact, during apoptosis, DRP1 has been shown to accumulate on mitochondrial tubules (Frank et al., 2001; Karbowski et al., 2002; Breckenridge et al., 2003; Germain et al., 2005), suggesting that apoptotic signals control its recruitment and/or dissociation from the mitochondrial membrane. However, the molecular details of this event are unknown. In this study, we use FRAP of the mitochondrial YFP-DRP1 puncta as well as biochemical recruitment experiments to gain insight into the cycling dynamics of DRP1 in healthy and apoptotic cells. The data show that the increased association of DRP1 with the mitochondrial membranes that has been observed during apoptosis is not caused by an increase in the recruitment of DRP1. Instead, the membrane-associated pool of DRP1 becomes irreversibly locked on the membrane during cell death in an hFis1-independent but Bax/Bak-dependent manner. The shift from rapid cycling early in apoptosis to stable mitochondrial association observed after fragmentation is accompanied by the stable sumoylation of DRP1, an event that is also dependent on the presence of Bax/Bak. This is the first study describing specific Bax/Bak-dependent biochemical transitions in DRP1 properties that link the induction of cell death to the initiation of changes in mitochondrial membrane dynamics.

Results

YFP-DRP1 cycles rapidly between the cytosol and preexisting sites on the mitochondrial membranes

In an effort to uncover the mechanisms of DRP1 association with mitochondrial membranes, we examined the dynamic properties of this event using FRAP (Fig. 1). GFP-Dnm1p has been shown to rescue the null mutant in *Saccharomyces cerevisiae* (Sesaki and Jensen, 1999; Legesse-Miller et al., 2003; Schauss et al., 2006), and fluorescently tagged DRP1 has been used extensively in worm and mammalian studies to examine the properties of this GTPase (Labrousse et al., 1999; Frank et al., 2001; Smirnova et al., 2001; Harder et al., 2004; Lee et al., 2004; Germain et al., 2005). Therefore, we constructed the YFP-DRP1 fusion protein and confirmed that it is recruited into punctate structures on the mitochondria similar to the endogenous protein (Fig. 1 A). The association of YFP-DRP1 with membranes is dynamic, as indicated by the efficient kinetics of FRAP (half-time = 50 s; Fig. 1 B). The cytosol rather than mitochondrial membranes constitutes the major supplier of unbleached fluorophores because the recovery is observed even when entire organelles are photobleached (unpublished data). The recovery of YFP-DRP1 fluorescence to the mitochondria is limited to ~80%, indicating that a portion of the membrane-associated protein cannot be replaced by unbleached molecules (Fig. 1 B). This immobile DRP1 population may represent a scaffold that is stably associated with the mitochondrial membrane. Consistent with this, we occasionally notice fluorescence recovery to the same puncta, suggesting that at least a portion of DRP1 is recruited to predetermined sites (Fig. 1 C). The small

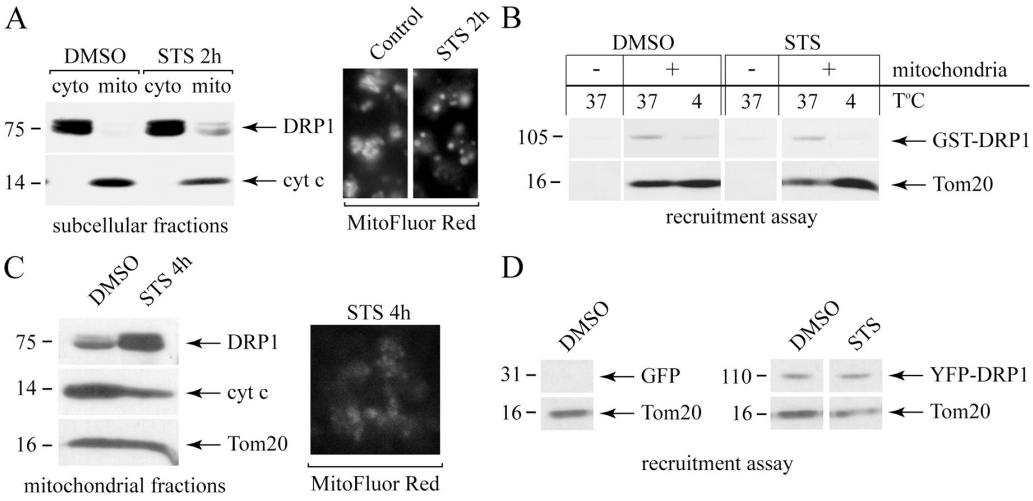

Figure 2. **The in vitro recruitment of recombinant DRP1 is not enhanced during apoptosis.** (A) Cytosolic and mitochondrial fractions purified from sHeLa cells treated with DMSO or STS for 2 h were subjected to SDS-PAGE, transferred to nitrocellulose, and blotted with antibodies against DRP1 and cytochrome *c* (cyt c; left). Mitochondrial fractions were incubated at 37°C with the MitoFluor dye to monitor the presence of mitochondrial $\Delta\Psi$ (right). (B) Mitochondrial fractions characterized in A were incubated with cytosol and GST-DRP1 for 1 h at the indicated temperatures. After the incubation, the reactions were centrifuged through a sucrose cushion to recover membranes, which were subsequently resolved by SDS-PAGE. Western blots revealed that GST-DRP1 and Tom20 associated with pelleted mitochondrial fractions. (C) Mitochondrial fractions purified from sHeLa cells treated with DMSO or STS for 4 h were subjected to SDS-PAGE, transferred to nitrocellulose, and blotted with antibodies against DRP1, cytochrome *c* (cyt c), and Tom20 (left). The same membrane fractions were incubated at 37°C with the MitoFluor red dye to monitor the presence of mitochondrial $\Delta\Psi$ (right). (D) Mitochondrial fractions characterized in C were incubated at 37°C with cytosol purified from DMSO or STS-treated cells expressing GFP or YFP-DRP1. The reactions were centrifuged through a sucrose cushion to recover membrane-associated proteins, which were subsequently resolved by SDS-PAGE. Western blots revealed that YFP-DRP1 and Tom20 associated with mitochondrial fractions.

size of the YFP-DRP1 puncta combined with the high mobility of the organelles complicates quantitative analysis of the frequency of recovery to the same puncta, although it is clear that many of these sites are conserved during the bleaching and recovery process.

In vitro recruitment of the recombinant DRP1 to mitochondrial membranes is not enhanced during apoptosis

Biochemical fractionation and immunofluorescence experiments indicate that DRP1 accumulates on mitochondrial membranes during apoptosis (Fig. 2, A and C; Frank et al., 2001; Karbowski et al., 2002; Breckenridge et al., 2003; Germain et al., 2005). However, it has not been demonstrated whether this accumulation is caused by increased recruitment of DRP1 from the cytosol or stabilization of existing membrane-associated DRP1 complexes. To explore this question, we performed in vitro recruitment experiments using mitochondria-enriched membrane fractions purified from untreated or staurosporin (STS)-treated suspension HeLa (sHeLa) cells (Fig. 2). Purified mitochondria retained cytochrome *c* (Fig. 2, A and C) and maintained $\Delta\Psi$, as revealed by the accumulation of a potential-sensitive dye, MitoFluor red (Fig. 2, A and C). As expected, mitochondria isolated from apoptotic cells contained higher levels of DRP1 on the membrane (Fig. 2, A and C; Frank et al., 2001; Karbowski et al., 2002; Breckenridge et al., 2003; Germain et al., 2005). Experiments were performed in the presence of nontreated cytosol or cytosol purified from apoptotic cells to ensure that accessory factors potentially necessary for DRP1 recruitment were present in the reaction mix. Purified GST-DRP1 was recruited to the mitochondrial membranes in a temperature-sensitive manner, confirming the specificity of the reaction (Fig. 2 B). Surprisingly, in vitro, the capacity of apoptotic mitochondria to recruit GST-DRP1 was comparable with that of the nontreated mitochondria (Fig. 2 B). Similar results were obtained using cytosol from sHeLa cells expressing YFP-DRP1 as a source of the recombinant protein and mitochondrial fractions purified from cells that have been treated with STS for longer periods of time (Fig. 2, C and D). Thus, accumulation of DRP1 on the mitochondrial membrane during apoptosis is not caused by an increase in the intrinsic capacity of mitochondria to recruit DRP1 from cytosol.

YFP-DRP1 fluorescence recovery to mitochondrial membranes is inhibited during apoptosis

Next, we assessed the cycling properties of YFP-DRP1 during apoptosis in vivo using FRAP. As reported previously, we noticed an accumulation of DRP1 on the mitochondrial membranes during apoptosis (Frank et al., 2001; Breckenridge et al., 2003), resulting in puncta that appear larger and brighter (compare Fig. 1 A with Fig. 3, A and C). Strikingly, we observed a complete block in the fluorescence recovery of YFP-DRP1 in HeLa cells treated with STS or anti-Fas–activating antibodies (Fig. 3). In fact, the mobile fraction of membrane-associated YFP-DRP1 decreased abruptly from 80 ± 15% in nontreated cells to 12 ± 5% in STS- and anti-Fas–treated cells (compare Fig. 1 B with Fig. 3, B and D). Thus, in apoptotic cells, YFP-DRP1 puncta appear very stable and are not subjected to rapid turnover, as observed in the steady state. Based on the biochemical recruitment experiments (Fig. 2) and on the FRAP

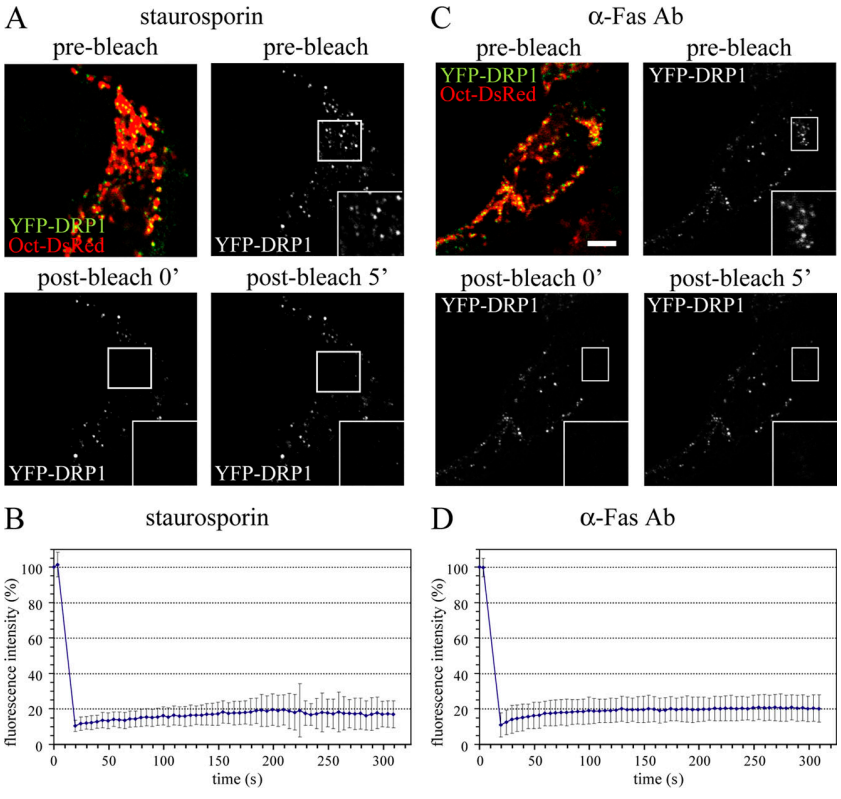

Figure 3. **YFP-DRP1 fluorescence recovery to mitochondrial membranes is inhibited during apoptosis.** (A and C) HeLa cells cotransfected with YFP-DRP1 and Oct-DsRed (overlay) were treated with STS or with anti-Fas–activating antibodies for the indicated amounts of time. The boxed regions (insets) were photobleached (0 min), and fluorescence recovery was monitored over time (5 min). (B and D) Relative fluorescence intensity of YFP-DRP1 recorded during a photobleaching protocol was plotted as a function of time. FRAP curves from16 cells treated with STS for 90–240 min (B) and from 15 cells treated with anti-Fas antibodies for 180–315 min (D) were used to generate mean plots. Error bars represent SD. Bar, 5 μm.

data, we conclude that DRP1 recruited during cell death becomes irreversibly locked on the membrane, eventually leading to the saturation of membrane-associated loci and an overall block in cycling.

To position the block in DRP1 cycling in the series of apoptotic events, we plotted the maximal values of fluorescence recovery from 42 cells as a function of time after STS treatment (Fig. 4 A). The data revealed that the block in cycling is a relatively synchronous event within the total population of cells. Photobleaching of YFP-DRP1 showed that 85% of cells treated from 0 to 70 min with STS displayed a maximal fluorescence recovery to mitochondrial puncta. There was much more variability between 70 and 110 min of STS treatment, with some cells recovering to 95% but others showing a sharp decrease of fluorescence recovery to only 10% of the prebleach levels. After 120 min of STS treatment, the recovery was reduced to <35% of prebleach levels of YFP-DRP1. In addition, examination of the videos from these 42 photobleaching experiments revealed that YFP-DRP1 fluorescence recovered to mitochondria undergoing fission (Fig. 4, B and B′; and Video 1, available at http://www.jcb.org/cgi/content/full/jcb.200610042/DC1). Thus, actively cycling DRP1 participates in fission during apoptosis-induced fragmentation. Conversely, fluorescence recovery of YFP-DRP1 was blocked in cells displaying fragmented and immotile mitochondria (Fig. 4, C and C′; and Video 2). The mitochondrial $\Delta\Psi$ was maintained in these cells, as indicated by the mitochondrial accumulation of MitoFluor red (Fig. 4 C′). Altogether, these data indicate that the block in YFP-DRP1 cycling occurs after mitochondrial fragmentation but before the loss of $\Delta\Psi$.

To position the block in DRP1 recycling relative to cytochrome *c* release, we fixed HeLa cells at 0, 30, 60, 90, 120, 150, and 180 min after STS treatment and immunostained with anti–cytochrome *c* antibodies. The percentage of cells displaying cytochrome *c* release from the mitochondria was scored, and the data were directly compared with the time course of maximal fluorescence recovery of YFP-DRP1 (Fig. 4 A). The release of cytochrome *c* was observed only in 10% of cells at the time when DRP1 becomes trapped on the mitochondrial membrane (80–100 min after STS treatment). This indicates that the transition in DRP1 cycling occurs before outer membrane permeabilization, supporting the data obtained from live cells demonstrating that the transition precedes the loss of $\Delta\Psi$. Finally, the transition did not require caspase activity because the general caspase inhibitor z-Val-Ala-Asp(OMe)-fluoromethyl ketone (zVAD-fmk; or the caspase 3 inhibitor V) did not affect the transition in DRP1 cycling, only inhibiting events downstream of outer mitochondrial membrane permeabilization (Figs. 3 and 4).

hFis1 is not required for DRP1 recycling at steady state and during apoptosis

The aforementioned data indicate that YFP-DRP is actively cycling during apoptotic fragmentation. To test whether fragmentation is mechanistically required for changes in DRP1 association with the membrane, we blocked mitochondrial fission by silencing hFis1 using a siRNA approach. The knockdown was confirmed by Western blotting and indirect immunofluorescence (Fig. 5 A). We then transfected hFis1 siRNA-treated cells with YFP-DRP1 and performed photobleaching studies on cells either untreated ($n = 10$) or treated with STS for >150 min ($n = 10$). In untreated hFis1-silenced cells, YFP-DRP1 fluorescence recovered within the same time frame as in wild-type (WT) cells (compare Fig. 1 B with Fig. 5, B and C), which is consistent with previous evidence that hFis1 is not required for the recruitment of DRP1 at the steady state (Lee et al., 2004; Stojanovski et al., 2004). Upon treatment with STS, we noticed a block in YFP-DRP1 recovery comparable with WT cells (compare

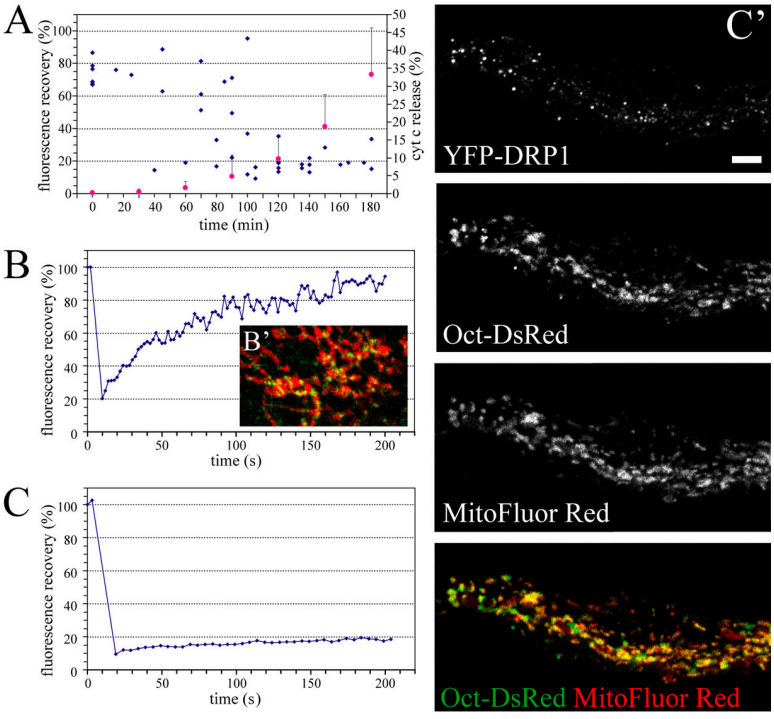

Figure 4. **The apoptotic block in YFP-DRP1 cycling occurs after fragmentation but before the loss of mitochondrial membrane potential.** (A) Scatter plot representing maximal fluorescence recovery recorded during a FRAP protocol in 42 cells expressing YFP-DRP1 as a function of time of treatment with STS (blue diamonds). Pink circles represent the percentage of cells showing cytosolic cytochrome *c* as determined by indirect immunofluorescence at different times of STS treatment. Values are means of three independent experiments. Error bars represent SD. (B) A FRAP plot from a cell treated for 100 min with STS expressing YFP-DRP1 (green) and Oct-DsRed (red; B′). Mitochondria display a characteristic beads-on-a-string appearance, indicating active fragmentation (B′ and Video 1, available at http://www.jcb.org/cgi/content/full/jcb.200610042/DC1). (C and C′) A FRAP plot (C) from a cell treated for 120 min with STS expressing YFP-DRP1 and Oct-DsRed (green; C′). Fragmented mitochondria are labeled with MitoFluor red (red), indicating the presence of $\Delta\Psi$ (C′). Video 2 illustrates the lack of mitochondrial movement after fragmentation. Bar, 5 μm.

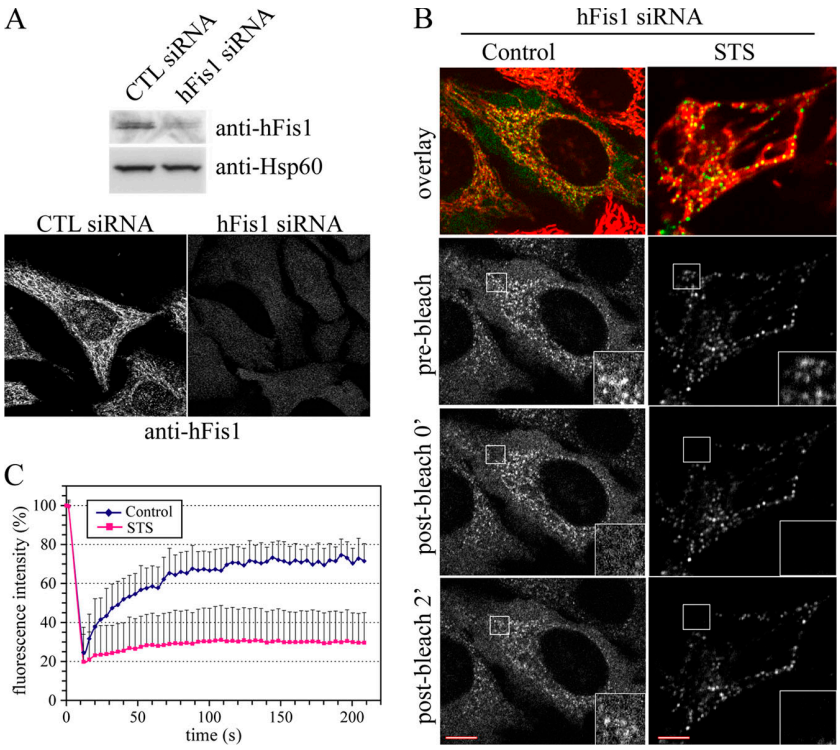

Figure 5. **hFis1 is not required for YFP-DRP1 recycling at steady state or during apoptosis.** (A) Control or specific siRNAs were used to silence the expression of hFis1 in HeLa cells, as shown by Western blotting and by indirect immunofluorescence with antibodies directed against hFis1. Antibodies against Hsp60 were used as a loading control (top). (B) hFis1 siRNA–treated Hela cells transfected with YFP-DRP1 were untreated or treated with 1 μM STS for >150 min. The overlay shows YFP-DRP1 (green) and a mitochondrial staining with MitoFluor red (red). Note the interconnected mitochondrial tubules in STS-treated cells. The boxed regions (insets) were photobleached (0 min), and fluorescence recovery was monitored over time (2 min). Bars, 5 μm. (C) Relative fluorescence intensity of YFP-DRP1 recorded during the photobleaching protocol was plotted as a function of time. FRAP curves from hFis1 siRNA–treated cells incubated with control media (n = 9) or with media containing STS for 150–250 min (n = 10) were used to generate mean plots. Error bars represent SD.

Fig. 3 B with Fig. 5, B and C). Interestingly, given that hFis1 inhibits mitochondrial fragmentation, the transition in YFP-DRP1 cycling was observed upon mitochondria that remained highly tubulated (7/10 photobleached cells; Fig. 5 B, STS overlay). The remaining three cells displayed an arrest in YFP-DRP1 cycling on partially fragmented mitochondria. This delayed fragmentation is likely caused by residual hFis1 present in RNAi-treated cells, as the silencing efficiency was ~70–80%. Together, these data indicate that fragmentation events that precede the trapping of DRP1 on the membrane are not required for the transition to occur and that hFis1 is not involved in the mechanisms that stabilize the mitochondrial association of DRP1.

The arrest in YFP-DRP1 cycling correlates with Bax translocation to the mitochondrial membrane and is Bax/Bak dependent

Because hFis1, a known component of the mitochondrial fission machinery, was not required for the stable association of DRP1 with mitochondria during cell death, we examined the potential role of the apoptotic machinery in this transition. Bax translocation from the cytosol to the mitochondrial membrane is an early apoptotic event that correlates with mitochondrial fragmentation and cytochrome *c* release (Frank et al., 2001; Karbowski et al., 2002; Germain et al., 2005). To determine when the cycling of DRP1 is altered relative to Bax translocation, we cotransfected CFP-Bax and YFP-DRP1 and monitored DRP1 cycling by FRAP before, during, and after STS-stimulated Bax translocation (Fig. 6). As soon as Bax puncta became detectable on the mitochondria, we observed colocalization between CFP-Bax and YFP-DRP1 as reported previously (Fig. 6, B′ and C′; Karbowski et al., 2002). YFP-DRP1 recovery at that time was comparable with that of untreated cells (Fig. 6 B). However, as Bax puncta on the mitochondria became more prominent, we noticed a sharp drop in the fluorescence recovery of YFP-DRP1 (Fig. 6 C). We grouped the results from multiple bleaching experiments into two categories: the first one examined the recycling of YFP-DRP1 in STS-treated cells displaying a cytosolic distribution of CFP-Bax (n = 9), and the second one regrouped apoptotic cells showing the mitochondrial recruitment of CFP-Bax (n = 17). As indicated in Fig. 6 D, the recovery of YFP-DRP1 in apoptotic cells with cytosolic CFP-Bax was comparable with untreated cells. In contrast, the block in YFP-DRP1 recycling was clearly observed in STS-treated cells in which CFP-Bax was mitochondrial (Fig. 6 D). Thus, the block in cycling of YFP-DRP1 correlates with Bax translocation to the mitochondria.

To determine whether the proapoptotic proteins Bax and Bak are necessary for the transition in DRP1 cycling, we monitored the fluorescence recovery of YFP-DRP1 in WT or Bax/Bak double knockout (DKO) baby mouse kidney (BMK) cells (Degenhardt et al., 2002). As observed by FRAP, the mobility of YFP-DRP1 in nontreated BMK DKO cells was comparable with that in WT cells, suggesting that Bax and Bak are not necessary for normal DRP1 cycling (unpublished data). To assess YFP-DRP1 cycling properties during apoptosis, STS treatment periods longer than 3 h were chosen to ensure that most cells were past the transition point mapped in Fig. 4 A. As expected, the fluorescence recovery of YFP-DRP1 was drastically reduced in apoptotic BMK WT cells, similar to HeLa cells (Fig. 7 A, left; and quantification in B). However, the kinetics of fluorescence recovery in BMK DKO cells were comparable with those in nonapoptotic cells, indicating that Bax/Bak are required for the block in DRP1 cycling (observed recovery in STS-treated

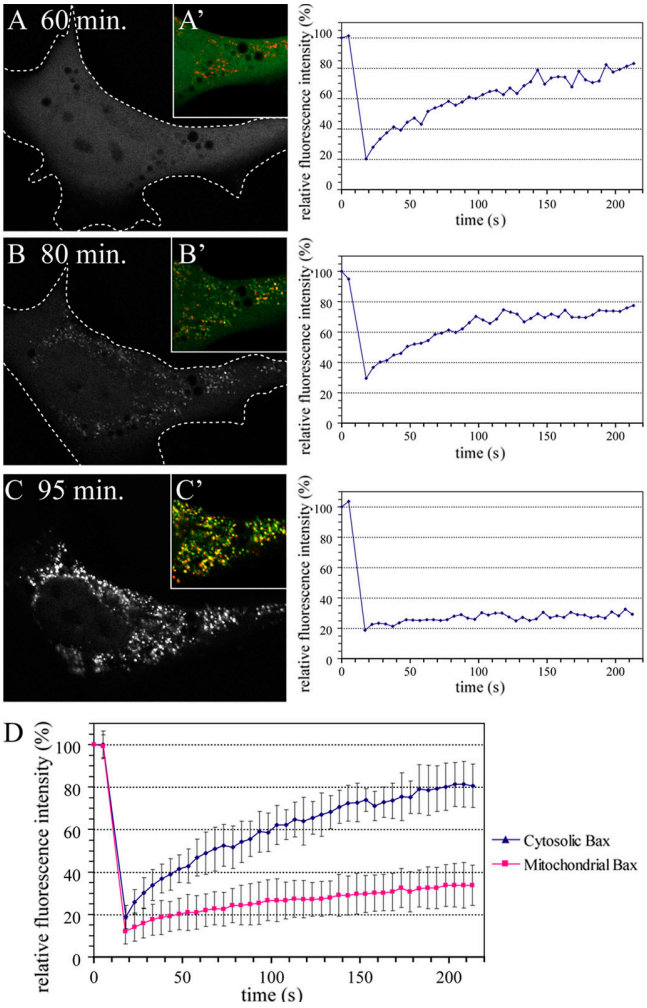

Figure 6. **The arrest in YFP-DRP1 cycling correlates with Bax translocation to the mitochondrial membrane.** (A–C) HeLa cells coexpressing YFP-DRP1 and CFP-Bax were treated with STS for 20–120 min before photobleaching. The distribution of CFP-Bax in a representative cell is documented on the left, whereas the fluorescence recovery of YFP-DRP1 in the same cell is shown on the right. Insets (A′–C′) show colocalization between YFP-DRP1 (red) and CFP-Bax (green). The dotted lines in A and B show the outlines of one cell. (D) Averaged FRAP curves showing the cycling of YFP-DRP1 in cells displaying the cytosolic (triangles; $n = 11$) or mitochondrial (squares; $n = 17$) distribution of CFP-Bax treated with STS for 20–120 min. Error bars represent SD.

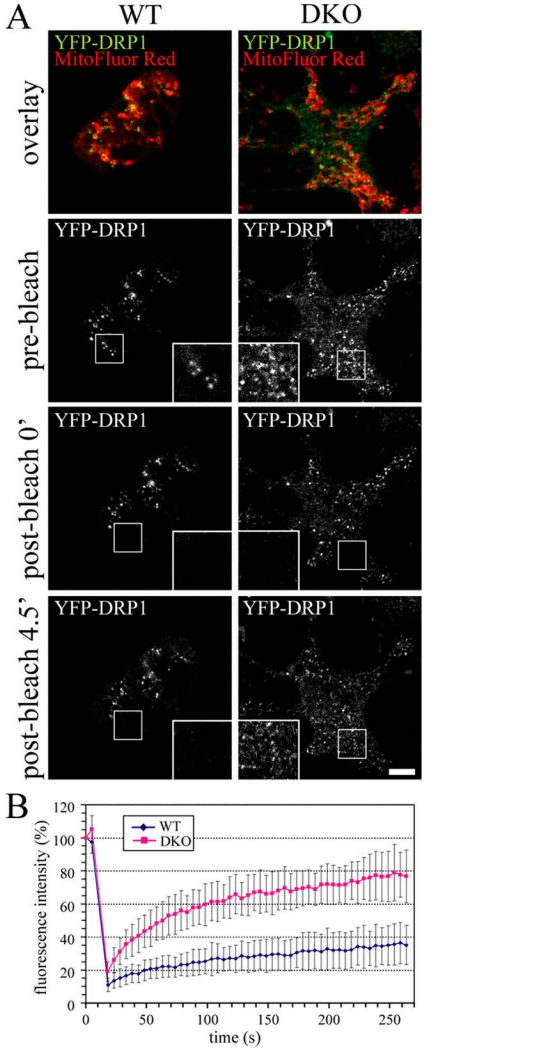

Figure 7. **The block in cycling of YFP-DRP1 during apoptosis is Bax/Bak dependent.** (A) Wild-type (WT) and Bax/Bak double knockout (DKO) BMK cells were transfected with YFP-DRP1 and treated with STS for 195–365 min before photobleaching. The boxed regions containing YFP-DRP1 (green) associated with mitochondria (red) was photobleached (0 min), and fluorescence recovery was monitored over time (4.5 min; insets). Bar, 5 μm. (B) Averaged FRAP curves showing the cycling of YFP-DRP1 in WT (diamonds; $n = 12$) and Bax/Bak knockout cells (DKO; squares; $n = 14$) treated with STS for 195–365 min. Error bars represent SD.

DKO cells is ∼80%, as in control cells [Fig. 1 B], with a half-time of 55 vs. 50 s in control cells; Fig. 1 B).

By subcellular fractionation, the association of DRP1 with mitochondrial membranes was similar in nontreated WT and DKO cells, confirming that at steady state, Bax and Bak do not modulate the membrane-binding properties of DRP1 (Fig. 8 A). Conversely, the increased membrane association of DRP1 characteristic of apoptotic WT cells was not detected in DKO cells, indicating that Bax/Bak are required for the stabilization of DRP1 on the mitochondrial membrane (Fig. 8 A).

DRP1 is sumoylated during apoptosis in a Bax/Bak-dependent manner

The apoptotic stimulus not only induced a stable membrane-associated form of DRP1 but also promoted the appearance of a high molecular weight DRP1-reactive band in cytosolic and mitochondrial fractions isolated from BMK cells (Fig. 8 A). Strikingly, the emergence of this high molecular weight species was absolutely dependent on the presence of Bax/Bak, as it was absent from STS-treated DKO cells (Fig. 8 A). We previously reported that DRP1 is transiently conjugated to small ubiquitin-like modifier-1 (SUMO-1) at steady state in COS-7 cells, resulting in the presence of a substoichiometric 150-kD band (Harder et al., 2004). In the present study, we also detected DRP1 conjugates at steady state in BMK cells (Fig. 8 A, cytosol; long exposure), and the absence of Bax/Bak did not affect the overall pattern of these substoichiometric conjugates. To determine whether the apoptotic-induced Bax/Bak-dependent band was indeed the result of an increase in sumoylation, we immunoprecipitated DRP1 from BMK cell extracts treated or untreated with STS.

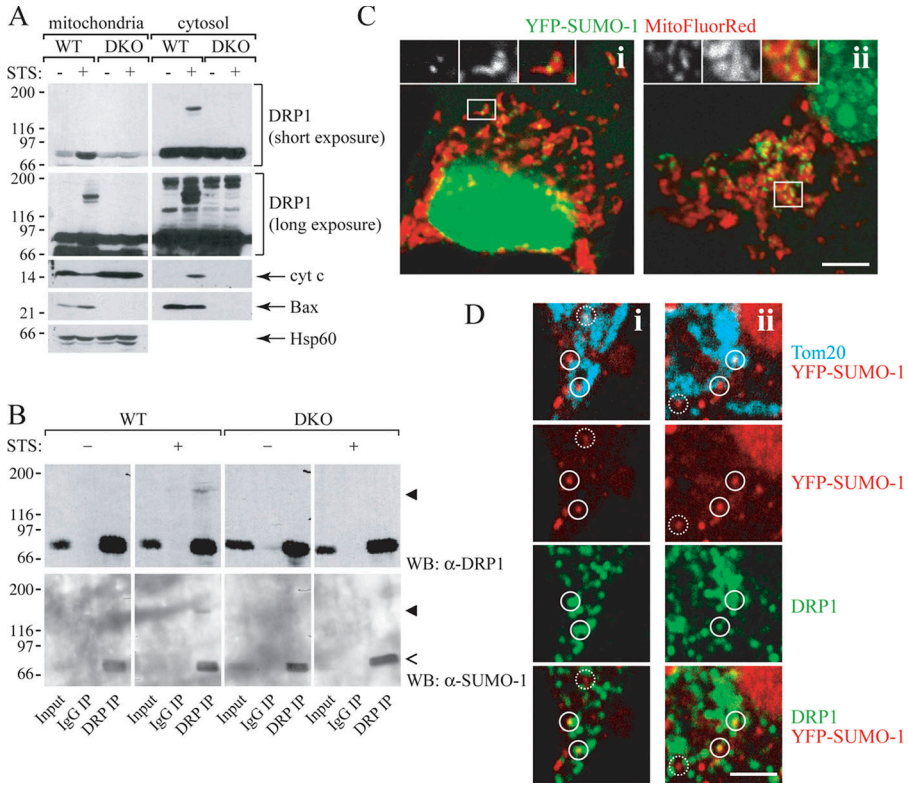

Figure 8. **DRP1 is sumoylated during apoptosis in a Bax/Bak-dependent manner.** (A) Mitochondrial and cytosolic fractions purified from BMK wild-type (WT) or Bax/Bak double knockout (DKO) cells treated with DMSO or STS for 4 h were subjected to SDS-PAGE, transferred to nitrocellulose, and blotted with antibodies against DRP1 and cytochrome *c* (cyt c), Bax, and Hsp60. Long exposure reveals a 150-kD band recognized by the anti-DRP antibody. (B) Total lysates from BMK WT and DKO cells were subjected to immunoprecipitation with total mouse IgG or anti-DRP1 antibodies. Specifically bound proteins were resolved by SDS-PAGE, transferred to nitrocellulose, and blotted with antibodies against DRP1 and SUMO-1. Input represents 5% of the total lysate used for immunoprecipitation. Closed arrowheads point to bands at 150 kD that are immunoreactive for both DRP1 and SUMO-1. Open arrowhead points to the monosumoylated DRP1. (C, i and ii) HeLa cells were transfected with YFP–SUMO-1 and treated with STS from 95 to 205 min. YFP–SUMO-1–positive puncta (red; left insets) were detected in association with mitochondria labeled with MitoFluor red (green; middle insets), often at potential fission sites (right insets). The insets show magnifications of the boxed regions. The left inset is a grayscale image of the YFP–SUMO-1 channel (shown in green in the overlay in the right inset), and the middle inset shows a grayscale image of the Mitofluor red channel (indicated in red in the overlay in the right inset). Note the presence of YFP–SUMO-1 at the sites of mitochondrial constriction. (D, i and ii) HeLa cells transfected with YFP–SUMO-1 (red) were treated with STS for 2 h, fixed, and immunostained with antibodies against Tom20 (blue) and DRP1 (green). YFP–SUMO-1 puncta associated with mitochondria are observed to colocalize (solid circles) or not colocalize (dotted circles) with DRP1. Bars (C), 5 μm; (D) 1 μm.

The DRP1-reactive 150-kD band detected in the immunoprecipitates was indeed labeled by anti–SUMO-1 antibodies, confirming its identity as a DRP1–SUMO-1 conjugate (Fig. 8 B).

To confirm the involvement of sumoylation during apoptosis-induced mitochondrial fragmentation, we determined the localization of YFP–SUMO-1 in live HeLa cells treated with STS. We have previously observed YFP–SUMO-1 association with mitochondria under steady-state conditions (Harder et al., 2004). However, given the lability and substoichiometric amounts of the conjugate at steady state, this is not easily detectable. Strikingly, upon the stimulation of cell death, YFP–SUMO-1 was readily observed to accumulate at sites of mitochondrial constriction and at mitochondrial tips (Fig. 8 C). This accumulation was observed during active apoptotic fragmentation as well as after fragmentation (Fig. S2, available at http://www.jcb.org/cgi/content/full/jcb.200610042/DC1). In addition, we observed partial colocalization between mitochondria-associated endogenous DRP1 and YFP–SUMO-1 during apoptotic death (Fig. 8 D). The lack of YFP–SUMO-1 from some DRP1-positive puncta likely reflects the transitory and substoichiometric nature of this posttranslational modification (as demonstrated in biochemical fractionation experiments; Fig. 8 A). Interestingly, the absence of DRP1 from some YFP–SUMO-1–positive puncta indicates the existence of additional mitochondrial SUMO-1 substrates as previously reported (Harder et al., 2004).

Finally, we wanted to examine whether the stable sumoylation of DRP1 was specific for apoptosis or whether this conjugation event was common to other treatments that induce nonapoptotic mitochondrial fragmentation or remodeling. As expected, treatment of BMK cells with STS induced the DRP1 conjugate, whereas incubation with carbonyl cyanide m-chlorophenylhydrazone or oligomycin (Legros et al., 2002; De Vos et al., 2005) did not trigger the appearance of high molecular weight DRP1 bands (Fig. S3, available at http://www.jcb.org/cgi/content/full/jcb.200610042/DC1). Together, these data demonstrate that the sumoylation of DRP1 is specifically stimulated during apoptosis in a manner dependent on Bax/Bak.

Discussion

In mammalian cells, the assembly dynamics of the mitochondrial fission complex are unknown. In this study, we document the cycling properties of DRP1 at steady state and during apoptotic death. Using FRAP, we demonstrate that the cytosolic DRP1 protein binds reversibly to membranes in healthy cells. Its cycling kinetics are comparable with those of human dynamin 2 at the centrosome (half-time = 60 s; Thompson et al., 2004). Interestingly, the yeast orthologue of DRP1, Dnm1p, was shown to recycle in a slow and inefficient manner, which may reflect important differences in the mechanisms of recruitment and retention of these two proteins (Legesse-Miller et al., 2003). Association of DRP1 with mitochondrial membranes appears more stable than that of many other proteins recruited to intracellular membranes. For example, examination of multiple

components of the exocyst machinery in yeast revealed two separate classes of proteins: those with time constants ranging from 12 to 23 s (Sec4p, Sec5p, Sec6p, Sec8p, Sec10p, Sec15p, and Exo84p) and those with a time constant of ∼60 s (Sec3p and Exo70p; Boyd et al., 2004). Coated vesicle components GGA1, clathrin, COPI, and Arf1 have been reported to recycle with half-times of recovery of ∼10–35 s (Wu et al., 2001; Presley et al., 2002; Puertollano et al., 2003). Therefore, the cycling kinetics of DRP1 is slower compared with other membrane-associated protein complexes. Interestingly, we also observed that the fluorescence recovery of DRP1 often occurred at pre-existing sites, indicating that DRP1 or its mitochondrial receptors generate stable membrane domains.

Several lines of evidence indicate that DRP1 plays an important role in the efficient progression of apoptosis (for review see Martinou and Youle, 2006). However, mechanisms that are responsible for regulation of the mitochondrial fission machinery during cell death are unknown. In this study, we define two phases of DRP1 cycling during apoptosis. The first phase is characterized by active DRP1 cycling and is independent of Bax/Bak, whereas the second phase is characterized by a stable membrane association of DRP1 that is Bax/Bak dependent. The combined biochemical and FRAP data suggest that the mitochondrial accumulation of DRP1 observed during the second phase results from stabilization of the membrane-bound protein rather than the stimulation of DRP1 recruitment (Frank et al., 2001; Breckenridge et al., 2003; for review see Martinou and Youle, 2006). This change in DRP1 properties occurs after Bax translocation to the membrane and depends on the presence of Bax/Bak, revealing that DRP1 not only functions downstream of Bax but that DRP1 cycling is regulated by Bax.

There are several mechanisms through which Bax/Bak could affect the membrane binding of DRP1. After the induction of apoptosis, Bax-positive puncta appear at fission sites, where they colocalize with DRP1 just before the block in cycling (Fig. 6). Therefore, Bax recruitment and oligomerization at DRP1 foci may directly or indirectly induce a shift in DRP1 cycling dynamics and promote its stable association with membranes. Interestingly, a BAR (Bin/amphiphysin/Rvs) domain–containing fission protein, endophilin B1/Bif-1, is known to bind to Bax and was recently shown to be required for Bax activation and membrane recruitment during apoptosis (Takahashi et al., 2005). As endophilin B1/Bif-1 function is required upstream of Bax, it would also be requisite for the transition in DRP1 cycling. It is possible that a stabilized microdomain induced by endophilin B1/Bif-1 bound to activated Bax oligomers may create an environment in which DRP1 is stably recruited. In turn, the constricting ability of DRP1 may also contribute to the formation of curvature within the outer membrane that is required for the efficient insertion of Bax (Basanez et al., 1999, 2002; Annis et al., 2005). Together, the recruitment of these proteins would create a stable microdomain that strengthens itself with a positive feedback mechanism. Evidence that the dominant-negative DRP1 delays (but does not block) Bax activation is consistent with this idea (Neuspiel et al., 2005). In the absence of Bax, these microdomains would instead be dynamic and transient, with DRP1 rapidly cycling on and off the membrane. In addition, Bax may induce changes in the calcium flux from the ER, which has been shown to be a required event for DRP1 recruitment and cristae remodeling (Breckenridge et al., 2003; Germain et al., 2005). The molecular details of these pathways remain to be explored, but our data show a substantial Bax/Bak-dependent transition in the nature of DRP1 puncta on the mitochondria during cell death.

It has been suggested that hFis1 functions as a receptor/adaptor for DRP1 in mitochondrial fission (Yoon et al., 2003; Yu et al., 2005). However, the FRAP data reported here demonstrate that hFis1 is not required for DRP1 cycling on and off membrane at steady state, which is consistent with previous observations in mammalian cells (Lee et al., 2004). This is distinct from yeast, in which Fis1p appears to function both upstream and downstream of Dnm1p recruitment (Mozdy et al., 2000; Tieu and Nunnari, 2000; Tieu et al., 2002; Cerveny and Jensen, 2003). Because the silencing of hFis1 results in a clear inhibition of mitochondrial fragmentation, it is more likely that hFis1 functions downstream of DRP1 recruitment in the fission process. This downstream function of hFis1 is consistent with the second requirement for yeast Fis1p in which, together with Mdv1p, they facilitate the oligomeric assembly of Dnm1p that is required to drive fission (Ingerman et al., 2005; Bhar et al., 2006; Naylor et al., 2006). Importantly, the silencing of hFis1 does not preclude the appearance of the transition in YFP-DRP1 cycling during apoptosis (Fig. 5). This is explained by the fact that Bax and caspase 3 activation, although slightly reduced, is still detectable in hFis1 knockdown cells (Fig. S1, available at http://www.jcb.org/cgi/content/full/jcb.200610042/DC1; and not depicted; Parone et al., 2006).

It is important to consider the function of the Bax/Bak-dependent stable membrane-associated form of DRP1. Our data indicate that the block in YFP-DRP1 cycling occurs after fragmentation and does not require mitochondrial fission because it is observed on tubulated mitochondria in the hFis1 siRNA-treated apoptotic cells (Fig. 5). Thus, it is likely that the function of YFP-DRP1 that is stably associated with membranes is unrelated to its role in mitochondrial fragmentation. Another important piece of data indicates that the block in cycling occurs before cytochrome *c* release and loss of $\Delta\Psi$. It has been shown that Bax oligomerization is required for permeabilization of the outer membrane (Antonsson et al., 2001; Annis et al., 2005) and that the remodeling of the inner membrane is required to facilitate the complete release of cytochrome *c* from intracristae stores (Scorrano et al., 2002; Germain et al., 2005; Cipolat et al., 2006; Frezza et al., 2006). Our previous study revealed that DRP1 plays a role in apoptosis because it is requisite not only for mitochondrial fission but also for cristae remodeling (Germain et al., 2005). Importantly, this DRP1-dependent remodeling requires a functional permeability transition pore (Germain et al., 2005), which is consistent with the appearance of a stable DRP1 form before the loss of $\Delta\Psi$ (Fig. 4). This suggests that the apoptosis-specific role for DRP1 may not reside in its ability to divide mitochondria but in the remodeling of both the inner and outer membranes that precedes the permeabilization of the outer membrane. Thus, we propose that during apoptosis, an actively cycling DRP1 mediates mitochondrial fission, whereas the Bax/Bak-dependent stable membrane-associated DRP1 is

involved in later apoptotic events, such as membrane remodeling that leads to the complete release of cytochrome *c* and eventual loss of $\Delta\Psi$.

Finally, we report a correlation between the stable association of DRP1 with the mitochondrial membranes and stimulation of the sumoylation of DRP1 during cell death. Importantly, both events are linked in their requirement for Bax/Bak, indicating that sumoylation may stabilize the association of DRP1 with mitochondrial membranes.

Posttranslational modification by SUMO commonly regulates the assembly and disassembly of protein complexes, protein localization, stability, and function (Johnson, 2004). Sumoylation is known to be highly substoichiometric because it often generates intermediates that result in new protein interactions or conformational states that persist even after SUMO removal (Johnson, 2004). Recent studies implicate SUMO as a regulator of nuclear localization and/or functions of proteins that are involved in apoptosis (Huang et al., 2003; Besnault-Mascard et al., 2005; Bischof et al., 2006; Hayashi et al., 2006; Janssen et al., 2006). In the present study, we report DRP1 as the first and only known mitochondrial SUMO target whose modification is up-regulated during apoptotic cell death. The detection of SUMO-positive dots associated with mitochondrial fission sites reinforces the notion that sumoylation plays a role in mitochondrial remodeling during apoptosis. Of note, the sumoylation of mitochondrial targets appears to be a selective rather than global event because overall mitochondria-associated sumoylation is not increased during apoptosis (unpublished data), indicating that specific proteins are being targeted, such as DRP1. Although we have documented the stimulation of DRP1 sumoylation, we have not provided evidence that this modification is functionally linked to DRP1 cycling during apoptosis. Our efforts to investigate this question have been complicated by the requirement to selectively block the second phase of DRP1 cycling and Bax/Bak-dependent sumoylation of DRP1. Further analysis of the role of sumoylation in DRP1 function during apoptosis will require a thorough characterization of its sumoylation/desumoylation cycle and of how it regulates the protein properties. Future work will focus on the dissection of specific Bax/Bak-dependent changes in DRP1 conjugation and cycling dynamics and their function in apoptotic membrane remodeling.

Materials and methods

Antibodies

Antibodies were obtained from the following providers: α-DRP1 (BD Biosciences), α-Hsp60 (Sigma-Aldrich), α–SUMO-1 (Zymed Laboratories), α-Bax (Upstate Biotechnology), α–cytochrome *c* (BD Biosciences), mouse IgG (Sigma-Aldrich), α-hFis1 (Biovision), and α-Tom20 rabbit serum (gift from G. Shore, McGill University, Quebec, Canada).

DNA constructs

YFP-DRP1, YFP–SUMO-1, and Oct-DsRed were described previously (Harder et al., 2004). pECFP-C3–human Bax was constructed using the pAdLoxGAL4-pEGFP-C3-hBax construct (gift from R. Slack, University of Ottawa, Ontario, Canada).

Cell culture

HeLa and BMK WT and DKO cells (gift from E. White, Rutgers University, New Brunswick, NJ) were grown in DME and RPMI 1640 medium (Invitrogen), respectively. sHeLa cells were maintained in F12 medium (Invitrogen) with 0.1 mM MEM nonessential amino acids (Invitrogen). For subcellular fractionation, sHeLa cells were grown in flasks for 5–6 d in 2 liters of MEM for suspension culture (Sigma-Aldrich) with 10 mM Hepes, pH 7.4, and 0.1 mM MEM nonessential amino acids. All media used were supplemented with 10% FBS and antibiotics.

Confocal microscopy

Cells grown on glass coverslips were transfected with LipofectAMINE 2000 (Invitrogen) according to the manufacturer's instructions. 16 h later, cells were treated with 1 μM STS (LC Laboratories) and 10 μM zVAD-fmk (MP Biomedicals) or with 1 μg/ml α-Fas–activating antibodies (Upstate Biotechnology), 40 μM caspase 3 inhibitor V (Calbiochem), and 10 μg/ml cycloheximide (Sigma-Aldrich). For live microscopy, cells were mounted in media with 20 mM Hepes, pH 7.4, and 50 nM MitoFluor red (Invitrogen) and were imaged at 37°C. For immunofluorescence, cells were fixed with 4% PFA/PBS for 15 min, permeabilized with 0.2% Triton X-100/PBS for 4 min, and blocked with 5% BSA, 5% FBS, and 0.02% Triton X-100 in PBS for 30 min at RT. Cells were labeled with primary antibodies and with goat α–rabbit Rhodamine X red and goat α–mouse AlexaFluor647 secondary antibodies (Invitrogen). Cells were visualized with a 100× NA 1.4 oil immersion objective (Olympus) at 1 airy U on a laser-scanning confocal microscope (IX80; Olympus) operated by FV1000 software version 1.4a (Olympus). To directly compare recovery curves from different treatments, data were normalized to correct for variations in background fluorescence (F_{bkgd}) and loss of fluorescence during the bleach according to the formula $F(t)_{norm} = 100 \times (F(t)_{ROI} - F_{bkgd})(F_{i\_cell} - F_{bkgd})/(F(t)_{cell} - F_{bkgd})(F_{i\_ROI} - F_{bkgd})$, where $F(t)_{ROI}$ = region of interest intensity, $F(t)_{cell}$ = total cell intensity at any given time point (t), F_{i_ROI} = initial intensity of the region of interest, and F_{i_cell} = initial intensity of the entire cell (Goodwin and Kenworthy, 2005). The resulting normalized data were then averaged for different cells, and the associated SD was calculated. The percent mobile fraction was calculated according to the formula $M_f = 100 \times (F_\infty - F_0)/(F_i - F_0)$, where F_∞, F_0, and F_i are the normalized fluorescence intensities at the asymptote, immediately after the bleach, and before the bleach, respectively (Goodwin and Kenworthy, 2005). Maximal fluorescence recovery at $t = \infty$ and half-time of recovery were calculated using nonlinear regression (curve fit) in Prism 4.03 software (GraphPad).

RNAi

Transfection of HeLa cells was performed using siGENOME SMARTpool transfection reagent (Dharmacon) according to the manufacturer's protocol. In brief, cells were seeded at 80% confluency in 10-cm dishes containing coverslips and transfected with either equal amounts of four siRNA oligonucleotides (hFis1; antisense sequences 5′-PUAACAGACCGCACAGCUCCUU-3′, 5′-PUUAGAUAGUACUGCAUGCCUU-3′, 5′-PUGAUGAAUGAUCUUUGAGCUU-3′, and 5′-PUGGCUGUUAAGCGUUUCUUUU-3′) or nontargeting sequence siRNA (glyceraldehyde-3-phosphate dehydrogenase) oligonucleotides. Cells were exposed to the transfection mixture for 16 h in complete OPTI-MEM medium + 10% FBS, at which time the transfection medium was replaced. 48 h after transfection, the cells were re-transfected in the same way. 96 h after the initial transfection, cells were collected and analyzed for hFis1 expression. YFP-DRP1 was transfected 16 h before analysis by indirect immunofluorescence or by FRAP.

Subcellular fractionation

Cells treated with DMSO or 1.0–1.5 μM STS were collected by trypsinization or centrifugation and lysed using a ball-bearing cell breaker in buffer A (220 mM mannitol, 68 mM sucrose, 80 mM KCl, 0.5 mM $Mg[CH_3COO]_2$, 10 mM Hepes, pH 7.4, 2 mg/ml BSA, and protease inhibitor cocktail [Roche Diagnostics]). Lysates were centrifuged at 3,000 rpm for 10 min at 4°C. The supernatant was spun at 10,000 rpm for 15 min at 4°C, yielding a mitochondria-enriched pellet and a light membrane fraction. Light membranes were spun at 70,000 rpm for 40 min at 4°C in a TLA 100.4 rotor (Beckman Coulter) to yield cytosol. Equal protein amounts from each fraction were analyzed by SDS-PAGE and Western blotting.

In vitro recruitment experiments

The assay was performed in a 50-μl volume with 50 μg of mitochondria and 50 μg of cytosol from sHeLa cells in the presence of 50–100 nM GST or GST-DRP1 in 110 mM mannitol, 70 mM sucrose, 80 mM KCl, 0.25 mM EGTA, 3 mM $Mg(CH_3COO)_2$, 15 mM Hepes, pH 7.4, 2 mM K_2HPO_4, 1 mM ATP(K^+), 0.08 mM ADP, 5 mM Na succinate, 1 mM DTT, and 1 mg/ml BSA. Soluble components were centrifuged before the assay at 80,000 rpm for 30 min at 4°C in a TLA 100.4 rotor (Beckman Coulter). Reactions were incubated for 1 h on ice or at 37°C with mild shaking and were spun

through 1 ml of 250 mM sucrose and 10 mM Hepes, pH 7.4, at 13,000 rpm for 20 min at 4°C. Membrane pellets were analyzed by SDS-PAGE. To prepare virally expressed GFP and YFP-DRP1, sHeLa cells were infected with adenoviruses at 22 plaque-forming units/cell (gifts from R. Slack). 48 h later, cells were treated with DMSO or 1 μM STS for 4 h and lysed by sonication in buffer A lacking BSA. The lysate was precleared for 5 min at 13,000 rpm, and the resulting supernatant was spun at 80,000 rpm for 40 min in a TLA 100.4 rotor. 10 μg of cytosol was used per recruitment reaction.

Fusion proteins

GST and GST-DRP1 were produced in an *Escherichia coli* BL21 strain. In brief, fusion proteins were induced with 0.5 mM IPTG at 22°C for 20 h. Bacteria were lysed in a French press in buffer B (20 mM Hepes, pH 7.4, 100 mM NaCl, 2 mM $MgCl_2$, 1 mM DTT, and protease inhibitors). The lysate was supplemented with 1% Triton X-100 and spun at 35,000 rpm for 30 min at 4°C in a Ti55.2 rotor (Beckman Coulter). The supernatant was incubated overnight with glutathione–Sepharose beads (GE Healthcare). Beads were washed in buffer B supplemented with 0.1% Triton X-100, and the fusion proteins were eluted from the beads according to a standard protocol.

Immunoprecipitation

BMK cells were treated with 1 μM STS or 0.01% DMSO for 4 h and scraped in 10 mM Hepes, pH 7.4, 50 mM NaCl, 2 mM $Mg(CH_3COO)_2$, 20 mM *N*-ethylmaleimide, and protease inhibitor cocktail. Cells were solubilized with 1% Triton X-100 and spun at 80,000 rpm in the TLA 100.4 rotor (Beckman Coulter). Precleared supernatant was incubated overnight with protein G–Sepharose beads (GE Healthcare) coupled to α-DRP1 antibody or total mouse IgG. Specifically bound proteins were resolved by SDS-PAGE and analyzed by Western blotting.

Online supplemental material

Supplemental videos and images within the figures were acquired on a laser-scanning confocal microscope (IX80 FV1000; Olympus). HeLa cells were transfected overnight with YFP-DRP1 or YFP–SUMO-1 and treated for 1 μM STS and 10 μM zVAD-fmk, respectively. For imaging, cells were mounted in a chamber in DME media supplemented with 20 mM Hepes, pH 7.4, and 50 nM MitoFluor red (Invitrogen) at 37°C. Fig. S1 shows that apoptosis proceeds in cells silenced for the expression of hFis1. Fig. S2 shows that YFP–SUMO-1 is associated with apoptotic mitochondria during and after fragmentation. Fig. S3 shows that the stable SUMO-1 conjugate of DRP1 is specific to apoptotic fragmentation. Videos 1 and 2 show HeLa cells that were transfected with YFP-DRP1 and Oct-DsRed and treated with 1 μM STS. Videos 3 and 4 show HeLa cells expressing YFP–SUMO-1–positive puncta that were imaged in time-lapse microscopy to follow the mitochondria labeled with MitoFluor red. Online supplemental material is available at http://www.jcb.org/cgi/content/full/jcb.200610042/DC1.

We would like to thank Eileen White for the Bax/Bak DKO BMK cell lines, Eric Cheung and Ruth Slack for Bax reagents and technical advice, and Gordon Shore, Chris Harder, and members of the laboratory for advice and reading of the manuscript.

This work was supported by Canadian Institutes of Health Research (CIHR) operating grant 68833, a CIHR New Investigator Award to H.M. McBride, and a CIHR postdoctoral fellowship to S. Wasiak.

Submitted: 9 October 2006
Accepted: 4 April 2007

References

Annis, M.G., E.L. Soucie, P.J. Dlugosz, J.A. Cruz-Aguado, L.Z. Penn, B. Leber, and D.W. Andrews. 2005. Bax forms multispanning monomers that oligomerize to permeabilize membranes during apoptosis. *EMBO J.* 24:2096–2103.

Antonsson, B., S. Montessuit, B. Sanchez, and J.C. Martinou. 2001. Bax is present as a high molecular weight oligomer/complex in the mitochondrial membrane of apoptotic cells. *J. Biol. Chem.* 276:11615–11623.

Arnoult, D., N. Rismanchi, A. Grodet, R.G. Roberts, D.P. Seeburg, J. Estaquier, M. Sheng, and C. Blackstone. 2005. Bax/Bak-dependent release of DDP/TIMM8a promotes Drp1-mediated mitochondrial fission and mitoptosis during programmed cell death. *Curr. Biol.* 15:2112–2118.

Basanez, G., A. Nechushtan, O. Drozhinin, A. Chanturiya, E. Choe, S. Tutt, K.A. Wood, Y. Hsu, J. Zimmerberg, and R.J. Youle. 1999. Bax, but not Bcl-xL, decreases the lifetime of planar phospholipid bilayer membranes at subnanomolar concentrations. *Proc. Natl. Acad. Sci. USA*. 96:5492–5497.

Basanez, G., J.C. Sharpe, J. Galanis, T.B. Brandt, J.M. Hardwick, and J. Zimmerberg. 2002. Bax-type apoptotic proteins porate pure lipid bilayers through a mechanism sensitive to intrinsic monolayer curvature. *J. Biol. Chem.* 277:49360–49365.

Besnault-Mascard, L., C. Leprince, M.T. Auffredou, B. Meunier, M.F. Bourgeade, J. Camonis, H.K. Lorenzo, and A. Vazquez. 2005. Caspase-8 sumoylation is associated with nuclear localization. *Oncogene*. 24:3268–3273.

Bhar, D., M.A. Karren, M. Babst, and J.M. Shaw. 2006. Dimeric Dnm1-G385D interacts with Mdv1 on mitochondria and can be stimulated to assemble into fission complexes containing Mdv1 and Fis1. *J. Biol. Chem.* 281:17312–17320.

Bischof, O., K. Schwamborn, N. Martin, A. Werner, C. Sustmann, R. Grosschedl, and A. Dejean. 2006. The E3 SUMO ligase PIASy is a regulator of cellular senescence and apoptosis. *Mol. Cell*. 22:783–794.

Boyd, C., T. Hughes, M. Pypaert, and P. Novick. 2004. Vesicles carry most exocyst subunits to exocytic sites marked by the remaining two subunits, Sec3p and Exo70p. *J. Cell Biol.* 167:889–901.

Breckenridge, D.G., M. Stojanovic, R.C. Marcellus, and G.C. Shore. 2003. Caspase cleavage product of BAP31 induces mitochondrial fission through endoplasmic reticulum calcium signals, enhancing cytochrome *c* release to the cytosol. *J. Cell Biol.* 160:1115–1127.

Cerveny, K.L., and R.E. Jensen. 2003. The WD-repeats of Net2p interact with Dnm1p and Fis1p to regulate division of mitochondria. *Mol. Biol. Cell*. 14:4126–4139.

Chan, D.C. 2006. Mitochondrial fusion and fission in mammals. *Annu. Rev. Cell Dev. Biol*. 22:79–99.

Cipolat, S., T. Rudka, D. Hartmann, V. Costa, L. Serneels, K. Craessaerts, K. Metzger, C. Frezza, W. Annaert, L. D'Adamio, et al. 2006. Mitochondrial rhomboid PARL regulates cytochrome c release during apoptosis via OPA1-dependent cristae remodeling. *Cell*. 126:163–175.

De Vos, K.J., V.J. Allan, A.J. Grierson, and M.P. Sheetz. 2005. Mitochondrial function and actin regulate dynamin-related protein 1-dependent mitochondrial fission. *Curr. Biol.* 15:678–683.

Degenhardt, K., R. Sundararajan, T. Lindsten, C. Thompson, and E. White. 2002. Bax and Bak independently promote cytochrome c release from mitochondria. *J. Biol. Chem.* 277:14127–14134.

Frank, S., B. Gaume, E.S. Bergmann-Leitner, W.W. Leitner, E.G. Robert, F. Catez, C.L. Smith, and R.J. Youle. 2001. The role of dynamin-related protein 1, a mediator of mitochondrial fission, in apoptosis. *Dev. Cell*. 1:515–525.

Frezza, C., S. Cipolat, O. Martins de Brito, M. Micaroni, G.V. Beznoussenko, T. Rudka, D. Bartoli, R.S. Polishuck, N.N. Danial, B. De Strooper, and L. Scorrano. 2006. OPA1 controls apoptotic cristae remodeling independently from mitochondrial fusion. *Cell*. 126:177–189.

Fukushima, N.H., E. Brisch, B.R. Keegan, W. Bleazard, and J.M. Shaw. 2001. The GTPase effector domain sequence of the Dnm1p GTPase regulates self-assembly and controls a rate-limiting step in mitochondrial fission. *Mol. Biol. Cell*. 12:2756–2766.

Germain, M., J.P. Mathai, H.M. McBride, and G.C. Shore. 2005. Endoplasmic reticulum BIK initiates DRP1-regulated remodelling of mitochondrial cristae during apoptosis. *EMBO J.* 24:1546–1556.

Goodwin, J.S., and A.K. Kenworthy. 2005. Photobleaching approaches to investigate diffusional mobility and trafficking of Ras in living cells. *Methods*. 37:154–164.

Griffin, E.E., J. Graumann, and D.C. Chan. 2005. The WD40 protein Caf4p is a component of the mitochondrial fission machinery and recruits Dnm1p to mitochondria. *J. Cell Biol.* 170:237–248.

Harder, Z., R. Zunino, and H. McBride. 2004. Sumo1 conjugates mitochondrial substrates and participates in mitochondrial fission. *Curr. Biol.* 14:340–345.

Hayashi, N., H. Shirakura, T. Uehara, and Y. Nomura. 2006. Relationship between SUMO-1 modification of caspase-7 and its nuclear localization in human neuronal cells. *Neurosci. Lett.* 397:5–9.

Heath-Engel, H.M., and G.C. Shore. 2006. Mitochondrial membrane dynamics, cristae remodelling and apoptosis. *Biochim. Biophys. Acta*. 1763:549–560.

Huang, T.T., S.M. Wuerzberger-Davis, Z.H. Wu, and S. Miyamoto. 2003. Sequential modification of NEMO/IKKgamma by SUMO-1 and ubiquitin mediates NF-kappaB activation by genotoxic stress. *Cell*. 115:565–576.

Ingerman, E., E.M. Perkins, M. Marino, J.A. Mears, J.M. McCaffery, J.E. Hinshaw, and J. Nunnari. 2005. Dnm1 forms spirals that are structurally tailored to fit mitochondria. *J. Cell Biol.* 170:1021–1027.

James, D.I., P.A. Parone, Y. Mattenberger, and J.C. Martinou. 2003. hFis1, a novel component of the mammalian mitochondrial fission machinery. *J. Biol. Chem.* 278:36373–36379.

Janssen, K., T.G. Hofmann, D.A. Jans, R.T. Hay, K. Schulze-Osthoff, and U. Fischer. 2006. Apoptin is modified by SUMO conjugation and targeted to promyelocytic leukemia protein nuclear bodies. *Oncogene*. 26:1557–1566.

Johnson, E.S. 2004. Protein modification by SUMO. *Annu. Rev. Biochem.* 73:355–382.

Karbowski, M., Y.J. Lee, B. Gaume, S.Y. Jeong, S. Frank, A. Nechushtan, A. Santel, M. Fuller, C.L. Smith, and R.J. Youle. 2002. Spatial and temporal association of Bax with mitochondrial fission sites, Drp1, and Mfn2 during apoptosis. *J. Cell Biol.* 159:931–938.

Karbowski, M., S.Y. Jeong, and R.J. Youle. 2004. Endophilin B1 is required for the maintenance of mitochondrial morphology. *J. Cell Biol.* 166:1027–1039.

Karbowski, M., K.L. Norris, M.M. Cleland, S.Y. Jeong, and R.J. Youle. 2006. Role of Bax and Bak in mitochondrial morphogenesis. *Nature*. 443:658–662.

Karren, M.A., E.M. Coonrod, T.K. Anderson, and J.M. Shaw. 2005. The role of Fis1p-Mdv1p interactions in mitochondrial fission complex assembly. *J. Cell Biol.* 171:291–301.

Labrousse, A.M., M.D. Zappaterra, D.A. Rube, and A.M. van der Bliek. 1999. *C. elegans* dynamin-related protein DRP-1 controls severing of the mitochondrial outer membrane. *Mol. Cell*. 4:815–826.

Lee, Y.J., S.Y. Jeong, M. Karbowski, C.L. Smith, and R.J. Youle. 2004. Roles of the mammalian mitochondrial fission and fusion mediators Fis1, Drp1, and Opa1 in apoptosis. *Mol. Biol. Cell*. 15:5001–5011.

Legesse-Miller, A., R.H. Massol, and T. Kirchhausen. 2003. Constriction and dnm1p recruitment are distinct processes in mitochondrial fission. *Mol. Biol. Cell*. 14:1953–1963.

Legros, F., A. Lombes, P. Frachon, and M. Rojo. 2002. Mitochondrial fusion in human cells is efficient, requires the inner membrane potential, and is mediated by mitofusins. *Mol. Biol. Cell*. 13:4343–4354.

Martinou, J.C., and R.J. Youle. 2006. Which came first, the cytochrome c release or the mitochondrial fission? *Cell Death Differ.* 13:1291–1295.

McBride, H.M., M. Neuspiel, and S. Wasiak. 2006. Mitochondria: more than just a powerhouse. *Curr. Biol.* 16:R551–R560.

Mishra, R.K., S.S. Jatiani, A. Kumar, V.R. Simhadri, R.V. Hosur, and R. Mittal. 2004. Dynamin interacts with members of the sumoylation machinery. *J. Biol. Chem.* 279:31445–31454.

Mozdy, A.D., J.M. McCaffery, and J.M. Shaw. 2000. Dnm1p GTPase-mediated mitochondrial fission is a multi-step process requiring the novel integral membrane component Fis1p. *J. Cell Biol.* 151:367–380.

Mukamel, Z., and A. Kimchi. 2004. Death-associated protein 3 localizes to the mitochondria and is involved in the process of mitochondrial fragmentation during cell death. *J. Biol. Chem.* 279:36732–36738.

Nakamura, N., Y. Kimura, M. Tokuda, S. Honda, and S. Hirose. 2006. MARCH-V is a novel mitofusin 2- and Drp1-binding protein able to change mitochondrial morphology. *EMBO Rep*. 7:1019–1022.

Naylor, K., E. Ingerman, V. Okreglak, M. Marino, J.E. Hinshaw, and J. Nunnari. 2006. Mdv1 interacts with assembled dnm1 to promote mitochondrial division. *J. Biol. Chem.* 281:2177–2183.

Neuspiel, M., R. Zunino, S. Gangaraju, P. Rippstein, and H.M. McBride. 2005. Activated Mfn2 signals mitochondrial fusion, interferes with Bax activation and reduces susceptibility to radical induced depolarization. *J. Biol. Chem.* 280:25060–25070.

Niemann, A., M. Ruegg, V. La Padula, A. Schenone, and U. Suter. 2005. Ganglioside-induced differentiation associated protein 1 is a regulator of the mitochondrial network: new implications for Charcot-Marie-Tooth disease. *J. Cell Biol.* 170:1067–1078.

Okamoto, K., and J.M. Shaw. 2005. Mitochondrial morphology and dynamics in yeast and multicellular eukaryotes. *Annu. Rev. Genet.* 39:503–536.

Parone, P.A., D.I. James, S. Da Cruz, Y. Mattenberger, O. Donze, F. Barja, and J.C. Martinou. 2006. Inhibiting the mitochondrial fission machinery does not prevent Bax/Bak-dependent apoptosis. *Mol. Cell. Biol.* 26:7397–7408.

Pitts, K.R., M.A. McNiven, and Y. Yoon. 2004. Mitochondria-specific function of the dynamin family protein DLP1 is mediated by its C-terminal domains. *J. Biol. Chem.* 279:50286–50294.

Presley, J.F., T.H. Ward, A.C. Pfeifer, E.D. Siggia, R.D. Phair, and J. Lippincott-Schwartz. 2002. Dissection of COPI and Arf1 dynamics in vivo and role in Golgi membrane transport. *Nature*. 417:187–193.

Puertollano, R., N.N. van der Wel, L.E. Greene, E. Eisenberg, P.J. Peters, and J.S. Bonifacino. 2003. Morphology and dynamics of clathrin/GGA1-coated carriers budding from the trans-Golgi network. *Mol. Biol. Cell*. 14:1545–1557.

Schauss, A.C., J. Bewersdorf, and S. Jakobs. 2006. Fis1p and Caf4p, but not Mdv1p, determine the polar localization of Dnm1p clusters on the mitochondrial surface. *J. Cell Sci.* 119:3098–3106.

Scorrano, L., M. Ashiya, K. Buttle, S. Weiler, S.A. Oakes, C.A. Mannella, and S.J. Korsmeyer. 2002. A distinct pathway remodels mitochondrial cristae and mobilizes cytochrome c during apoptosis. *Dev. Cell*. 2:55–67.

Sesaki, H., and R.E. Jensen. 1999. Division versus fusion: Dnm1p and Fzo1p antagonistically regulate mitochondrial shape. *J. Cell Biol.* 147:699–706.

Shin, H.W., H. Takatsu, H. Mukai, E. Munekata, K. Murakami, and K. Nakayama. 1999. Intermolecular and interdomain interactions of a dynamin-related GTP-binding protein, Dnm1p/Vps1p-like protein. *J. Biol. Chem.* 274:2780–2785.

Smirnova, E., L. Griparic, D.L. Shurland, and A.M. van Der Bliek. 2001. Dynamin-related protein drp1 is required for mitochondrial division in mammalian cells. *Mol. Biol. Cell*. 12:2245–2256.

Stojanovski, D., O.S. Koutsopoulos, K. Okamoto, and M.T. Ryan. 2004. Levels of human Fis1 at the mitochondrial outer membrane regulate mitochondrial morphology. *J. Cell Sci.* 117:1201–1210.

Takahashi, Y., M. Karbowski, H. Yamaguchi, A. Kazi, J. Wu, S.M. Sebti, R.J. Youle, and H.G. Wang. 2005. Loss of Bif-1 suppresses Bax/Bak conformational change and mitochondrial apoptosis. *Mol. Cell. Biol.* 25:9369–9382.

Thompson, H.M., H. Cao, J. Chen, U. Euteneuer, and M.A. McNiven. 2004. Dynamin 2 binds gamma-tubulin and participates in centrosome cohesion. *Nat. Cell Biol.* 6:335–342.

Tieu, Q., and J. Nunnari. 2000. Mdv1p is a WD repeat protein that interacts with the dynamin-related GTPase, Dnm1p, to trigger mitochondrial division. *J. Cell Biol.* 151:353–366.

Tieu, Q., V. Okreglak, K. Naylor, and J. Nunnari. 2002. The WD repeat protein, Mdv1p, functions as a molecular adaptor by interacting with Dnm1p and Fis1p during mitochondrial fission. *J. Cell Biol.* 158:445–452.

Tondera, D., F. Czauderna, K. Paulick, R. Schwarzer, J. Kaufmann, and A. Santel. 2005. The mitochondrial protein MTP18 contributes to mitochondrial fission in mammalian cells. *J. Cell Sci.* 118:3049–3059.

Wu, X., X. Zhao, L. Baylor, S. Kaushal, E. Eisenberg, and L.E. Greene. 2001. Clathrin exchange during clathrin-mediated endocytosis. *J. Cell Biol.* 155:291–300.

Yonashiro, R., S. Ishido, S. Kyo, T. Fukuda, E. Goto, Y. Matsuki, M. Ohmura-Hoshino, K. Sada, H. Hotta, H. Yamamura, et al. 2006. A novel mitochondrial ubiquitin ligase plays a critical role in mitochondrial dynamics. *EMBO J.* 25:3618–3626.

Yoon, Y., K.R. Pitts, and M.A. McNiven. 2001. Mammalian dynamin-like protein dlp1 tubulates membranes. *Mol. Biol. Cell*. 12:2894–2905.

Yoon, Y., E.W. Krueger, B.J. Oswald, and M.A. McNiven. 2003. The mitochondrial protein hFis1 regulates mitochondrial fission in mammalian cells through an interaction with the dynamin-like protein DLP1. *Mol. Cell. Biol.* 23:5409–5420.

Yu, T., R.J. Fox, L.S. Burwell, and Y. Yoon. 2005. Regulation of mitochondrial fission and apoptosis by the mitochondrial outer membrane protein hFis1. *J. Cell Sci.* 118:4141–4151.

Yu, T., J.L. Robotham, and Y. Yoon. 2006. Increased production of reactive oxygen species in hyperglycemic conditions requires dynamic change of mitochondrial morphology. *Proc. Natl. Acad. Sci. USA*. 103:2653–2658.

Zhu, P.P., A. Patterson, J. Stadler, D.P. Seeburg, M. Sheng, and C. Blackstone. 2004. Intra- and intermolecular domain interactions of the C-terminal GTPase effector domain of the multimeric dynamin-like GTPase Drp1. *J. Biol. Chem.* 279:35967–35974.